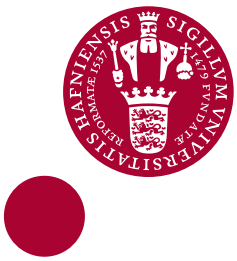

Reconfigured Cyanogenic Glucoside Biosynthesis in Eucalyptus cladocalyx Involves a Cytochrome P450 CYP706C55

Hansen, Cecilie Ida Cetti; Sørensen, Mette; Veiga, Thiago A. M.; Zibrandtsen, Juliane F.S.; Heskes, Allison M.; Olsen, Carl Erik; Boughton, Berin A.; Møller, Birger Lindberg; Neilson, Elizabeth Heather Jakobsen

Published in:
Plant Physiology

DOI:
10.1104/pp.18.00998

Publication date:
2018

Document version
Publisher's PDF, also known as Version of record

Reconfigured Cyanogenic Glucoside Biosynthesis in *Eucalyptus cladocalyx* Involves a Cytochrome P450 CYP706C55[1][OPEN]

Cecilie Cetti Hansen,[a,b] Mette Sørensen,[a,b] Thiago A.M. Veiga,[c] Juliane F.S. Zibrandtsen,[a,2] Allison M. Heskes,[a] Carl Erik Olsen,[a,b] Berin A. Boughton,[d] Birger Lindberg Møller,[a,b,e] and Elizabeth H.J. Neilson[a,b,3,4]

[a]Plant Biochemistry Laboratory, Department of Plant and Environmental Sciences, University of Copenhagen, 1871 Frederiksberg C, Copenhagen, Denmark
[b]VILLUM Center for Plant Plasticity, University of Copenhagen, 1971 Frederiksberg C, Copenhagen, Denmark
[c]Department of Chemistry, Federal University of São Paulo, Diadema 09972-270, Brazil
[d]Metabolomics Australia, School of BioSciences, University of Melbourne, Melbourne, Victoria 3010, Australia
[e]Center for Synthetic Biology, University of Copenhagen, 1871 Frederiksberg C, Copenhagen, Denmark

ORCID IDs: 0000-0002-0973-6466 (C.C.H.); 0000-0001-9787-8386 (M.S.); 0000-0002-1377-158X (T.A.V.); 0000-0001-5613-7362 (J.F.Z.); 0000-0002-2732-5185 (A.M.H.); 0000-0002-2275-0596 (C.E.O.); 0000-0001-6342-9814 (B.A.B.); 0000-0002-3252-3119 (B.L.M.); 0000-0002-8279-9906 (E.H.N.)

Cyanogenic glucosides are a class of specialized metabolites widespread in the plant kingdom. Cyanogenic glucosides are α-hydroxynitriles, and their hydrolysis releases toxic hydrogen cyanide, providing an effective chemical defense against herbivores. *Eucalyptus cladocalyx* is a cyanogenic tree, allocating up to 20% of leaf nitrogen to the biosynthesis of the cyanogenic monoglucoside, prunasin. Here, mass spectrometry analyses of *E. cladocalyx* tissues revealed spatial and ontogenetic variations in prunasin content, as well as the presence of the cyanogenic diglucoside amygdalin in flower buds and flowers. The identification and biochemical characterization of the prunasin biosynthetic enzymes revealed a unique enzyme configuration for prunasin production in *E. cladocalyx*. This result indicates that a multifunctional cytochrome P450 (CYP), CYP79A125, catalyzes the initial conversion of L-phenylalanine into its corresponding aldoxime, phenylacetaldoxime; a function consistent with other members of the CYP79 family. In contrast to the single multifunctional CYP known from other plant species, the conversion of phenylacetaldoxime to the α-hydroxynitrile, mandelonitrile, is catalyzed by two distinct CYPs. CYP706C55 catalyzes the dehydration of phenylacetaldoxime, an unusual CYP reaction. The resulting phenylacetonitrile is subsequently hydroxylatedby CYP71B103 to form mandelonitrile. The final glucosylation step to yield prunasin is catalyzed by a UDP-glucosyltransferase, UGT85A59. Members of the CYP706 family have not been reported previously to participate in the biosynthesis of cyanogenic glucosides, and the pathway structure in *E. cladocalyx* represents an example of convergent evolution in the biosynthesis of cyanogenic glucosides in plants.

Cyanogenic glucosides are a class of specialized metabolites found widespread in the plant kingdom. They are present in diverse taxa, including species in the genera *Pteridium* (monilophyte), *Taxus* (gymnosperm), *Sorghum* (monocot), *Manihot*, *Trifolium*, *Prunus*, and *Eucalyptus* (eudicots; Vetter, 2017). Upon tissue disruption, such as would be caused by herbivory, the cyanogenic glucoside is hydrolyzed by a specific β-glucosidase that cleaves off the sugar moiety. The resulting cyanohydrin dissociates, spontaneously or catalyzed by an α-hydroxynitrile lyase, resulting in the release of toxic hydrogen cyanide. This process is known as cyanogenesis (Gleadow and Møller, 2014). Their ability to release hydrogen cyanide makes cyanogenic glucosides chemical defense molecules against generalist herbivores and pathogens (Gleadow and Woodrow, 2002). Cyanogenic glucosides also have been shown to constitute a source of reduced nitrogen that is mobilized by endogenous turnover pathways (Pičmanová et al., 2015; Bjarnholt et al., 2018; Schmidt et al., 2018a).

The biosynthetic pathway genes for a cyanogenic glucoside were first identified and cloned from sorghum (*Sorghum bicolor*), which accumulates the Tyr-derived dhurrin (Koch et al., 1995; Bak et al., 1998; Jones et al., 1999). This provided a starting point for the identification of cyanogenic glucoside pathway genes in other plant species. The biosynthetic pathway for the Val-derived linamarin and Ile-derived lotaustralin has been elucidated from cassava (*Manihot esculenta*; Andersen et al., 2000; Jørgensen et al., 2011; Kannangara et al., 2011) and *Lotus japonicus* (Forslund et al., 2004; Takos et al., 2011), and recently, the full pathway for the Phe-derived diglucoside amygdalin from almond (*Prunus dulcis*) was identified (Thodberg et al., 2018). In species with characterized cyanogenic glucoside biosynthetic pathways, the production of monoglucosides involves two cytochrome P450s (CYPs) and a soluble UDP-glucosyltransferase (UGT). The first CYP is a member of the CYP79 family and catalyzes the conversion of an amino acid to the corresponding aldoxime. A CYP71 or CYP736 family member subsequently converts the aldoxime to a cyanohydrin. The labile cyanohydrin is stabilized by glucosylation to form the final cyanogenic glucosides in a reaction catalyzed by a UGT from

the UGT85 family. Work on dhurrin biosynthesis in sorghum shows that the two CYPs and UGT of the pathway form a metabolon enabling efficient channeling between enzymes that avoids the accumulation of toxic intermediates (Laursen et al., 2016; Bassard et al., 2017).

Eucalyptus is a large genus with over 800 species (Coppen, 2002). They are the world's most widely planted forest hardwood trees due to their fast growth, environmental plasticity, and exceptional wood properties (Myburg et al., 2014). The trees are grown for industrial purposes such as the production of pulp for paper, firewood, charcoal, and essential oils. *Eucalyptus* plants synthesize a broad spectrum of specialized metabolites, including terpenes, phenolics, formylated phloroglucinols, and cyanogenic glucosides (Eschler et al., 2000; Gleadow et al., 2008; Padovan et al., 2014; Marsh et al., 2017). Very little is known about the biosynthesis of specialized metabolites in *Eucalyptus* trees. The genome of *Eucalyptus grandis*, published in 2014 (Myburg et al., 2014), will potentially facilitate the identification of enzymes involved in these pathways. *E. grandis* has many tandem duplicated genes and tandem expanded clusters, as exemplified by the large number of terpene synthase genes (113) and the expansion of some phenylpropanoid genes (Myburg et al., 2014; Külheim et al., 2015). The significant expansion of some gene families in *Eucalyptus* species provides challenging obstacles toward the identification of pathway genes due to the large number of possible candidates.

More than 400 *Eucalyptus* species have been screened for cyanogenesis and 23 cyanogenic species have been identified, all containing prunasin as the major cyanogen (Fig. 1B; Gleadow et al., 2008). The South Australian species *Eucalyptus cladocalyx* (sugar gum) was first reported to be cyanogenic in 1928 (Finnemore and Cox, 1928), and a few years later, the foliar hydrogen cyanide source was identified as prunasin (Finnemore et al., 1935). In particular, the apical tips and young leaf tissue of *E. cladocalyx* can be highly cyanogenic, with up to 20% of leaf nitrogen allocated to prunasin biosynthesis (Gleadow et al., 1998; Gleadow and Woodrow, 2000b). Cyanogenic *Eucalyptus* species display unique ontogenetic variation. For example, *E. cladocalyx* has high levels of prunasin as a seedling compared with the adult, while the opposite trend is observed for *Eucalyptus yarraensis* and *Eucalyptus camphora* (Goodger et al., 2006; Neilson et al., 2011). As such, cyanogenic *Eucalyptus* species are an excellent system in which to investigate the regulation of chemical defense (Møller, 2010).

In this study, we investigate the spatial and ontogenetic variation and localization of cyanogenic glucoside accumulation in *E. cladocalyx*. Furthermore, we report the identification and functional characterization of the enzymes catalyzing the formation of prunasin from L-Phe in *E. cladocalyx*. We show that the conversion of Phe into the corresponding cyanohydrin requires the sequential action of three CYPs and includes the production of a free nitrile intermediate. One of the CYPs belongs to the CYP706 family, a family not reported previously to be involved in the synthesis of cyanogenic glucosides.

RESULTS

Spatial Distribution of Cyanogenic Glucosides

Prunasin extracts of expanded leaves from *E. cladocalyx* seedlings (4 months old), along with expanded leaves, immature flower buds, mature flower buds, flowers, and mature fruit from adult trees, were analyzed by liquid chromatography-mass spectrometry (LC-MS; Fig. 1). Prunasin was detected in all tissues examined. The lowest levels of prunasin were detected in young and adult leaves (17 ± 2.8 and 14 ± 4.2 μg mg^{-1} dry weight, respectively) and the highest levels were found in immature and mature flower buds (62 ± 12 and 53 ± 9 μg mg^{-1} dry weight, respectively), with intermediate levels detected in fruit (43 ± 1 μg mg^{-1} dry weight) and flowers (40 ± 1 μg mg^{-1} dry weight). Additionally, the diglucoside amygdalin (Fig. 1B) was found in the mature flower buds (4 ± 1.8 μg mg^{-1} dry weight) and flowers (9 ± 0.6 μg mg^{-1} dry weight),

[1]This research was supported by the "VILLUM Research Center for Plant Plasticity" (Project No. 7523), by the UCPH Excellence Program for Interdisciplinary Research to Center for Synthetic Biology, and by an ERC Advanced Grant (ERC-2012-ADG_20120314, Project No. 323034) to B.L.M. E.H.J.N. was supported by a Young Investigator Program fellowship from the VILLUM Foundation (Project No. 13167), a grant from the Carlsberg Foundation (Grant No. 2013_01_0908), and by a Danish Independent Research Council Sapere Aude Research Talent Post Doctoral Stipend (Grant No. 6111-00379B). T.A.M.V. was supported by a visiting professor fellowship from the Fundação de Amparo a Pesquisa do Estado de São Paulo (#FAPESP BPE 2014/11811-2). A.M.H. was supported by a Marie Skłodowska Curie Individual Fellowship (Project No. 658677). Mass spectrometry imaging was conducted at Metabolomics Australia located at the School of BioSciences, University of Melbourne, Australia, which is an NCRIS initiative under Bioplatforms Australia Pty Ltd.

[2]Current address: Syngenta, Crescent House, Tower Business Park, Manchester M20 2JE, UK.

[3]Author for contact: en@plen.ku.dk.

[4]Senior author.

The author responsible for distribution of materials integral to the findings presented in this article in accordance with the policy described in the Instructions for Authors (www.plantphysiol.org) is: Elizabeth H.J. Neilson (en@plen.ku.dk).

E.H.J.N. conceived the study and research plans; C.C.H., M.S., T.A.M.V., J.F.S.Z., and E.H.J.N. performed the experiments; E.H.J.N., B.L.M., A.M.H., and B.A.B. supervised experimental work; C.E.O. and B.A.B. provided technical assistance; C.C.H., M.S., and E.H.J.N. analyzed the data; C.C.H. wrote the draft with contributions from M.S., E.H.J.N., and B.L.M.; all authors reviewed and approved the final article.

[OPEN]Articles can be viewed without a subscription.

www.plantphysiol.org/cgi/doi/10.1104/pp.18.00998

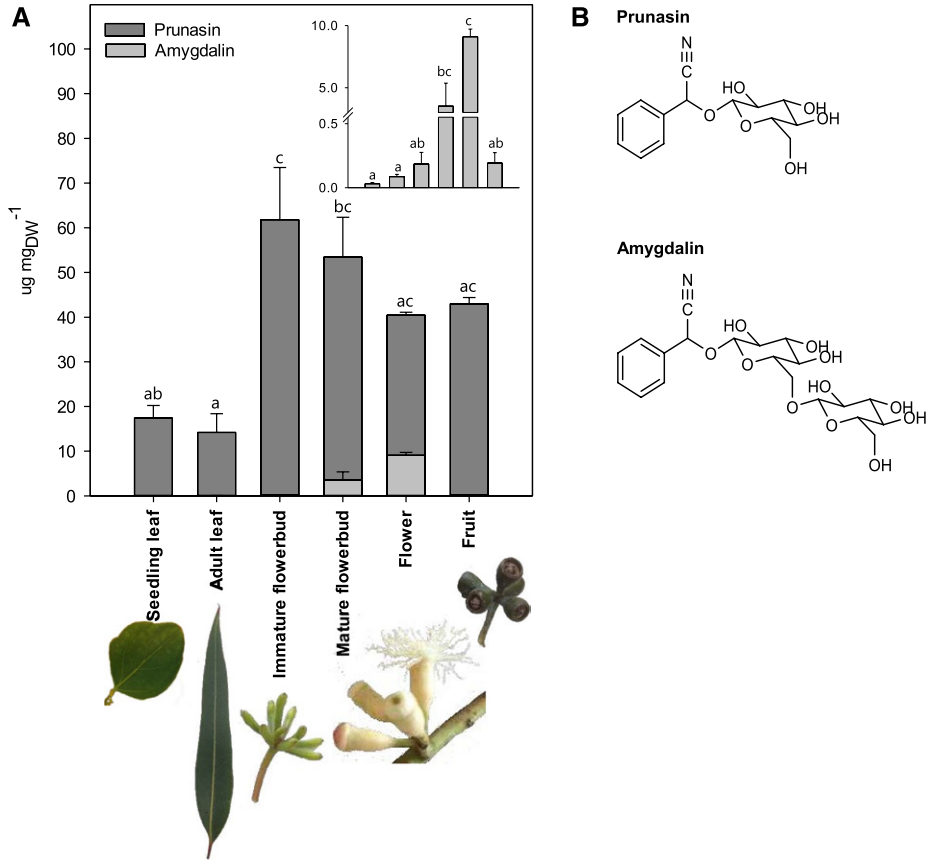

Figure 1. Prunasin and amygdalin accumulation in *E. cladocalyx*. A, Prunasin (dark gray) and amygdalin (light gray) content in expanded leaves from seedling and adult trees, immature and mature flower buds, flowers, and fruits. Bars represent means with SE. Magnified amygdalin concentrations are shown in the insert. Letters denote significance at $P < 0.05$ by one-way ANOVA. DW, Dry weight. B, Structures of prunasin and amygdalin.

accounting for approximately 6% and 18% of total cyanogenic content, respectively (Fig. 1A).

The use of matrix-assisted laser-desorption ionization-mass spectrometry imaging (MALDI-MSI) to map the spatial localization of prunasin and amygdalin within prepared tissues revealed prunasin to be localized to the mesophyll and vascular tissue of seedling and adult *E. cladocalyx* leaves (Fig. 2, A and B). Amygdalin was not detected in the leaf material using this method. MALDI-MSI of an *E. cladocalyx* flower bud demonstrated the presence of prunasin in the ground tissue of the ovary, hypanthium, and operculum as well as in filaments and anthers. Amygdalin was observed to be colocalized with prunasin, specifically in the filaments and staminal ring region (Fig. 2, C and D).

Phe Is the Precursor for Prunasin Synthesis in *E. cladocalyx*

Cyanogenic glucosides are known to be derived from amino acids (Gleadow and Møller, 2014); thus, we expected prunasin in *E. cladocalyx* to be derived from L-Phe, based on its structure (Fig. 1B). To verify this, L-[^{14}C]Phe was administered to apical tips, expanding leaves, and fully expanded leaves. All tested tissues demonstrated activity of the prunasin biosynthetic enzymes by the ability to synthesize prunasin from L-Phe (Fig. 3).

Identification and Testing of Three Candidate Genes Involved in Prunasin Biosynthesis

A candidate *CYP79* was identified by PCR, using cDNA generated from young leaves of *E. cladocalyx* and primers designed to the *E. yarraensis CYP79A34* (Neilson, 2012). Based on characterized cyanogenic glucoside biosynthetic pathways, candidate genes belonging to the CYP71 and UGT85 families that showed high expression in an *E. cladocalyx* transcriptome and no or very low expression in an acyanogenic *Eucalyptus globulus* transcriptome were identified (Spokevicius et al., 2017). Degenerate primers were designed to anneal to the untranslated regions of the *CYP71* and *UGT85* orthologs from the *E. grandis* genome available on Phytozome (Goodstein et al., 2012) and used

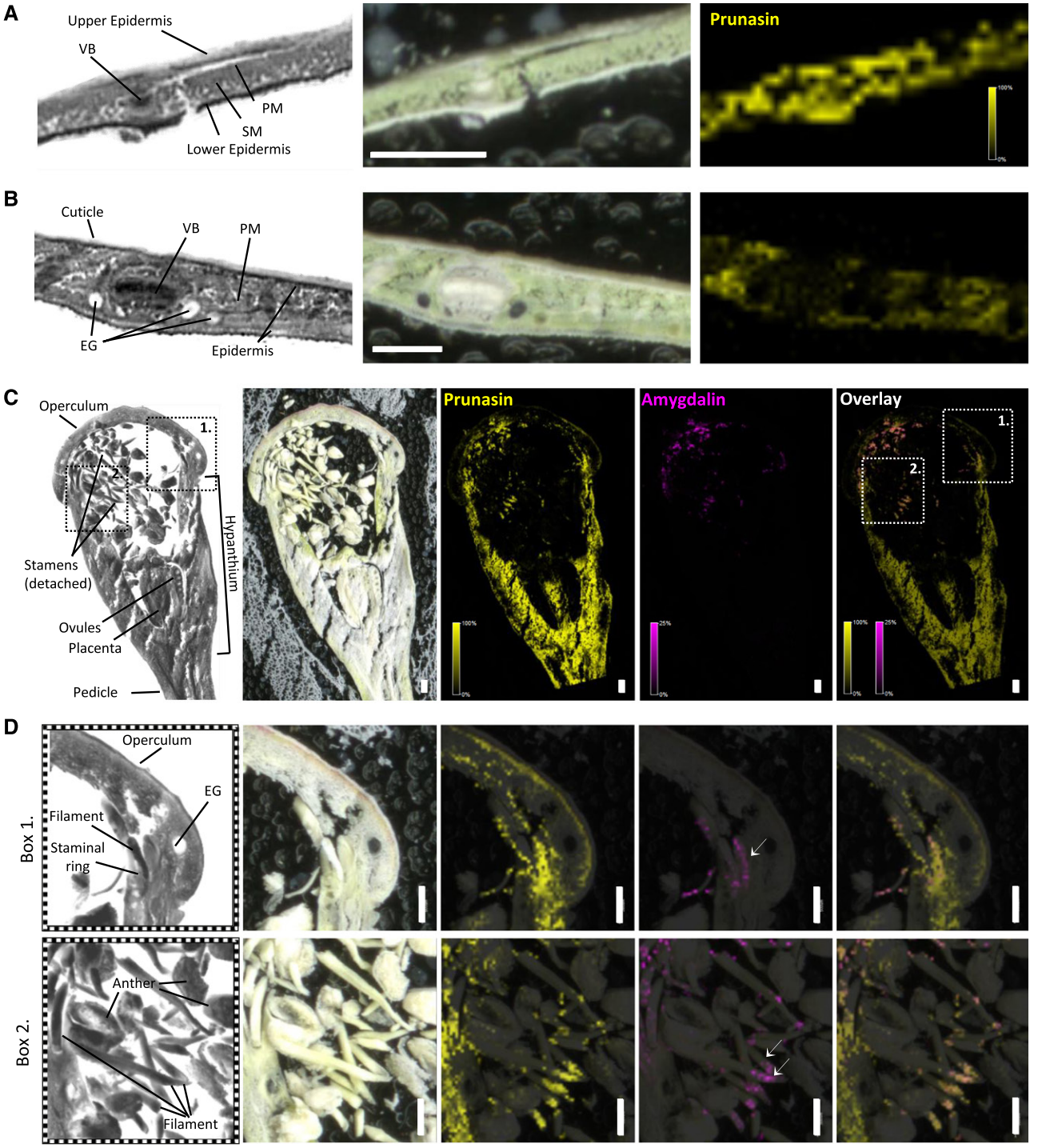

Figure 2. Localization of cyanogenic glucosides in *E. cladocalyx* tissue. A and B, Cross sections of seedling dorsoventral (A) and adult isobilateral (B) leaves prepared for MALDI-MSI, with corresponding ion maps of prunasin (yellow; mass-to-charge ratio [*m/z*] 334.0687; $[M+K]^+$) localizing to the mesophyll and vascular tissue. C, Longitudinal section of a flower bud prepared for MALDI-MSI, with corresponding ion maps of prunasin and amygdalin (pink; *m/z* 496.1216; $[M+K]^+$). D, Enlarged portions of the flower bud, with the section overlaid shown in the corresponding boxes 1 and 2. Prunasin ions were distributed in the ground tissue within the hypanthium, stamens, and operculum. Colocalization with amygdalin occurs in the filaments and around the staminal ring (indicated by white arrows). All images are root mean square normalized, with internal scaling of 100% for prunasin and 25% for amygdalin. EG, Embedded gland; PM, palisade; SM, spongy mesophyll; VB, vascular bundle. Bars = 500 μm.

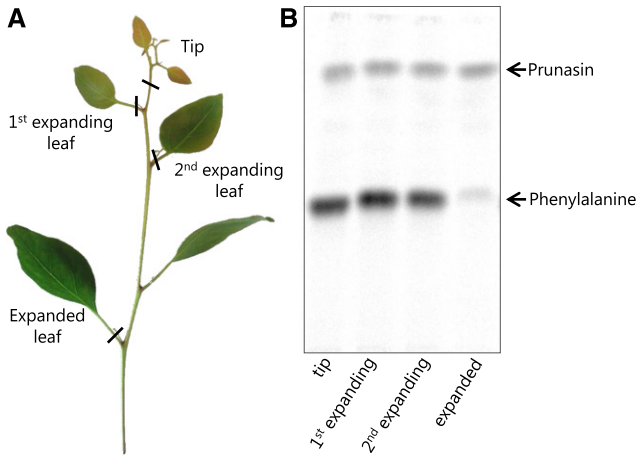

Figure 3. *E. cladocalyx* leaves of different developmental stages can synthesize prunasin from Phe. A, *E. cladocalyx* seedling withthe tissues used for administration with L-[^{14}C]Phe are indicated. B, Thin-layer chromatography (TLC) plate showing the production of prunasin from L-[^{14}C]Phe in apical tips, first and second expanding leaves, and fully expanded leaves.

to isolate the two gene sequences from *E. cladocalyx* cDNA. The CYPs where named CYP79A125 and CYP71B103 by David Nelson for the Standardized Cytochrome P450 Nomenclature Committee (Nelson, 2009), and the UGT candidate was named UGT85A59 according to the standard UGT Nomenclature Guidelines (Burchell et al., 1991; Mackenzie et al., 2005).

Testing of the three candidates by coinfiltration into *Nicotiana benthamiana* leaves resulted in the formation of only trace amounts of prunasin (Fig. 4A; Supplemental Fig. S1). The data, however, confirmed that CYP79A125 and UGT85A59 were functionally active in *N. benthamiana*. The expression of *CYP79A125* resulted in the production of glucosylated phenylacetaldoxime (Supplemental Fig. S2). This suggests that CYP79A125 can catalyze the conversion of L-Phe into phenylacetaldoxime that subsequently becomes glucosylated by endogenous *N. benthamiana* UGTs. The coexpression of *UGT85A59* showed an increase in glucosylated phenylacetaldoxime, demonstrating that UGT85A59 is active and able to glucosylate phenylacetaldoxime.

CYP706C55 Is Involved in Prunasin Biosynthesis

To identify other potential candidates involved in prunasin biosynthesis, a transcriptome was prepared from the highly cyanogenic and biosynthetically active apical tips of *E. cladocalyx*. *CYP71B103* and *CYP79A125* were the second and third most highly expressed CYPs, respectively, and *UGT85A59* was the highest expressed UGT. The most highly expressed CYP in the transcriptome belonged to the CYP706 family. This CYP706 was named CYP706C55 (Nelson, 2009) and selected for functional analysis.

CYP706C55 was tested by transient expression in *N. benthamiana* together with the previously identified pathway candidates. The expression of *CYP79A125*, *CYP706C55*, and *UGT85A59* resulted in small amounts of prunasin (Fig. 4A). However, the combined expression of all three CYP candidate genes with *UGT85A59* resulted in high accumulation of prunasin (Fig. 4A). Additionally, a novel peak with *m/z* 404 was observed and tentatively identified as a malonic acid ester of prunasin (Supplemental Fig. S3). Malonic acid derivatives have been observed previously upon transient expression in *Nicotiana* spp. (Tian and Dixon, 2006; Franzmayr et al., 2012; Ting et al., 2013), likely as a detoxification mechanism. No prunasin or derivatives thereof were observed in the negative control, where no *E. cladocalyx* genes were expressed. Likewise, no prunasin was observed upon the expression of *CYP71B103*, *CYP706C55*, and *UGT85A59*, confirming that CYP79A125 is required for prunasin production in *N. benthamiana*. Small amounts of prunasin were observed if the three CYPs were coexpressed, indicating that endogenous *N. benthamiana* glycosyltransferases can glycosylate the mandelonitrile to some extent. However, the prunasin levels increased 50-fold upon coexpression of *UGT85A59* (Fig. 4A).

To establish the order of the catalytic activity of CYP71B103 and CYP706C55 in prunasin biosynthesis, microsomes were prepared from infiltrated *N. benthamiana* leaves and assayed using radioactively labeled L-Phe as a substrate. Microsomes with CYP79A125 activity converted L-Phe into a product that comigrated with phenylacetaldoxime (Fig. 4B). Microsomes with CYP79A125 and CYP706C55 produced phenylacetaldoxime and phenylacetonitrile, and microsomes with all three CYPs showed the production of phenylacetaldoxime and mandelonitrile. Microsomes with CYP79A125 and CYP71B103 only produced phenylacetaldoxime, and the negative control without *E. cladocalyx* CYPs did not show any product formation.

In summary, based on transient expression analysis and microsomal assays, we demonstrate a route for prunasin biosynthesis in *E. cladocalyx* leaves. Specifically, CYP79A125 converts L-Phe into phenylacetaldoxime, which then is dehydrated into phenylacetonitrile by CYP706C55, hydroxylated by CYP71B103 to form mandelonitrile, and finally glucosylated by UGT85A59 to form prunasin (Fig. 4C).

Phylogenetic Analysis of the CYP79, CYP706, CYP736, and CYP71 Families

The amino acid sequences of CYP79A125, CYP706C55, and CYP71B103 were subjected to phylogenetic analysis together with functionally characterized CYP members from the CYP79, CYP706, CYP71, and CYP736 families (Fig. 5). These CYP families all contain at least one member involved in cyanogenic glucoside biosynthesis (Supplemental Table S1). All functionally characterized CYP79 members convert amino acids into their corresponding oximes (Sørensen et al., 2018),

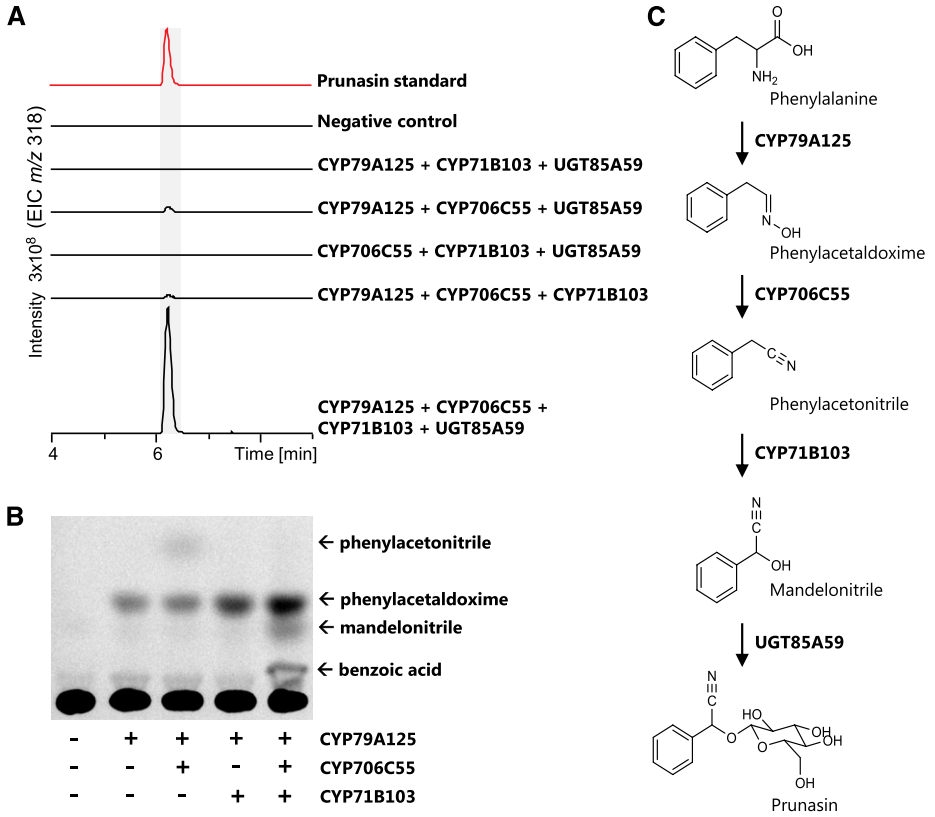

Figure 4. Prunasin biosynthesis is catalyzed by three CYPs and a UGT. A, LC-MS extracted ion chromatograms (EIC) for prunasin ($[M+Na]^+$ *m/z* 318) of *N. benthamiana* leaf extracts transiently expressing candidate genes. B, Microsomes prepared from *N. benthamiana* leaves transiently expressing candidate CYP genes were assayed with [^{14}C]Phe, and products were separated by TLC. C, Proposed pathway for prunasin synthesis in *E. cladocalyx*.

including 12 CYP79 members involved in cyanogenic glucoside biosynthesis. In contrast, members of the CYP71 family show broad functional diversity (Supplemental Table S1). The cyanogenic glucoside CYP71 members are distributed across several subfamilies, and this study introduces the first CYP71B involved in cyanogenic glucoside biosynthesis. Fewer CYPs belonging to the CYP706 and CYP736 families have been functionally characterized, with only a single member in each of the CYP706 and CYP736 families known to participate in cyanogenic glucoside biosynthesis.

Prunasin Accumulation through Leaf Ontogeny

The spatial variation of leaf prunasin was measured during plant development, and prunasin was extracted from apical tips, expanding leaves, and fully expanded leaves in plants at 4, 7, and 10 months of age. Quantitative variation in prunasin accumulation was observed throughout leaf ontogeny (Fig. 6A). The most cyanogenic tissue was the apical tips in 4-month-old plants. The accumulation of prunasin decreased with leaf age: in 4-month-old plants, prunasin accumulated to 45 ± 5 μg mg^{-1} dry weight in apical tips and decreased to 25 ± 2 μg mg^{-1} dry weight in expanding leaves and to 17 ± 3 μg mg^{-1} dry weight in fully expanded leaves. In older plants at 7 and 10 months of age, prunasin accumulation in leaves was lower and showed less variation between leaf types and plant age, not exceeding 11 μg mg^{-1} dry weight.

Expression of *CYP79A125*, *CYP71B103* and *CYP706C55* Is Positively Correlated

The expression of the characterized biosynthetic pathway genes was analyzed in apical tips and expanding and fully expanded leaves in plants at 4, 7, and 10 months of age (Fig. 6B). The expression of all genes was observed in all tested tissues, consistent with their ability to synthesize prunasin (Figs. 3 and 6A). Biological replicates showed a relatively large variation in expression; however, most individuals showed the same trend across tissues and time. In particular, all plants except one showed the lowest *CYP79A125* expression in expanded leaves at the three different time points. A Pearson correlation analysis revealed that the expression of the CYPs correlated: the expression of *CYP79A125* correlated with *CYP706C55* ($P < 0.01$) and *CYP71B103* ($P < 0.01$), and the expression of *CYP706C55* and *CYP71B103* also correlated ($P < 0.05$;

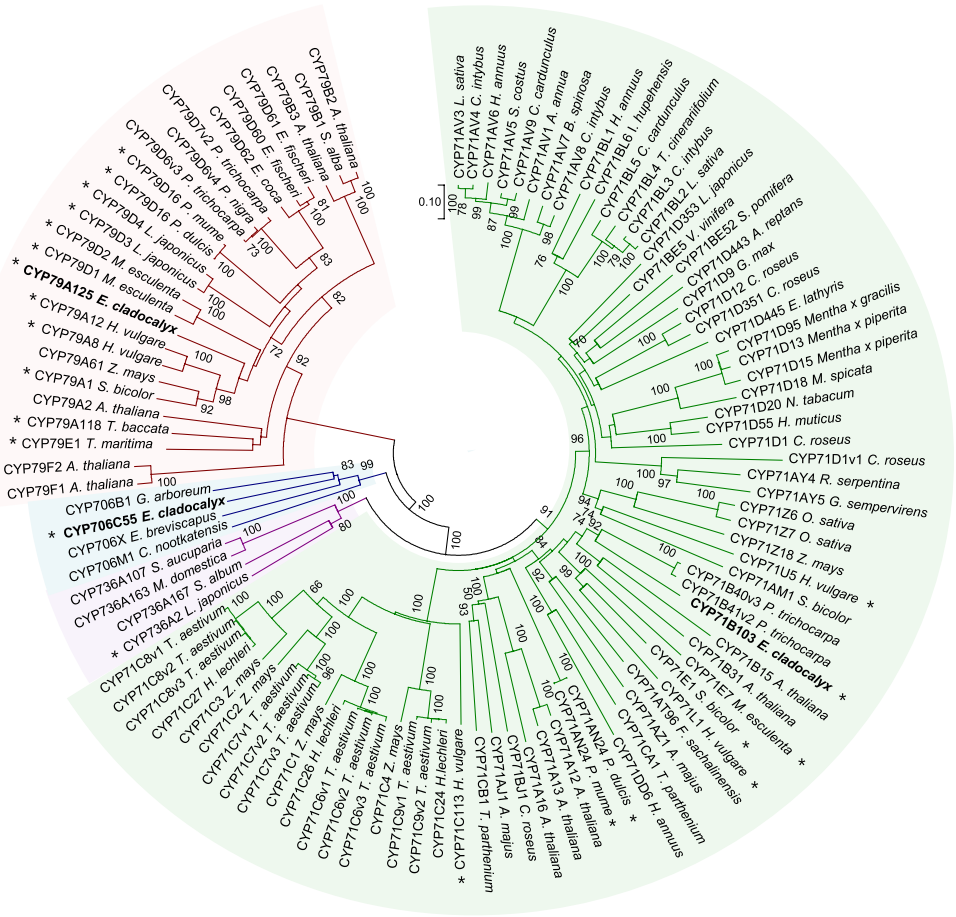

Figure 5. Phylogenetic analysis of functionally characterized CYPs belonging to the CYP79, CYP71, CYP706, and CYP736 families, including members involved in cyanogenic glucoside biosynthesis (indicated by asterisks). Phylogeny was inferred using the neighbor-joining method with n = 1,000 bootstrap replicates, with bootstrap values above 70 shown. The *E. cladocalyx* CYPs are marked in bold. Full species names, GenBank accession numbers, and references are listed in Supplemental Table S1.

Fig. 6C). In general, *UGT85A59* was highly expressed, and did not correlate with CYP expression.

DISCUSSION

Prunasin Accumulation Varies between Tissue Type and Plant Age

The accumulation of cyanogenic glucosides was investigated in different tissues of *E. cladocalyx* by LC-MS and MALDI-MSI. At the overall spatial level, the highest prunasin concentration (62 ± 12 μg mg^{-1} dry weight) was found in reproductive tissues (Fig. 1). In addition, *E. cladocalyx* leaf tissue was most cyanogenic in 4-month-old plants and then decreased with plant age; in particular, prunasin accumulation was found to decrease by leaf age, with apical tips being the most cyanogenic followed by expanding leaves and expanded leaves (Fig. 6). This is in agreement with a previous study observing relatively high cyanide potentials in flower buds, flowers, and fruits (Gleadow and Woodrow, 2000b) and reports showing that juvenile *E. cladocalyx* leaves are more cyanogenic than adult leaves, with the inverse relationship between leaf age and cyanogenic glucoside concentration (Gleadow and Woodrow, 2000b; Goodger et al., 2006). Only in young 1-week-old seedlings was prunasin content found to be insignificant (Gleadow and Woodrow, 2000b). We also identified the presence of the cyanogenic diglucoside amygdalin in *E. cladocalyx* (Fig. 1), with the highest levels in the flower buds and flowers (4 ± 2 and 9 ± 1 μg mg^{-1} dry weight, respectively). Amygdalin has not been reported previously to be present in *E. cladocalyx*. Cyanogenic diglucosides, including amygdalin, were identified in *E. camphora*, with the highest concentration also identified in reproductive tissue (Neilson et al., 2011).

Juvenile *E. cladocalyx* plants tend to be more cyanogenic compared with adult plants (Goodger et al., 2006). However, this is not the case in all cyanogenic *Eucalyptus* species, and the ontogenetic trajectory of cyanogenic glucoside production is known to differ between some species. In *E. camphora*, foliar cyanogenic glucoside production was found to increase with plant age, as prunasin accumulation increased from seedling to sapling to adult (Neilson et al., 2011). A similar pattern has been observed for *Eucalyptus polyanthemos* (Goodger et al., 2004). A different trajectory was observed for *E. yarraensis*, where a detailed study of prunasin concentration through ontogeny revealed that production increased gradually, with a maximum concentration at around 240 d after sowing; thereafter,

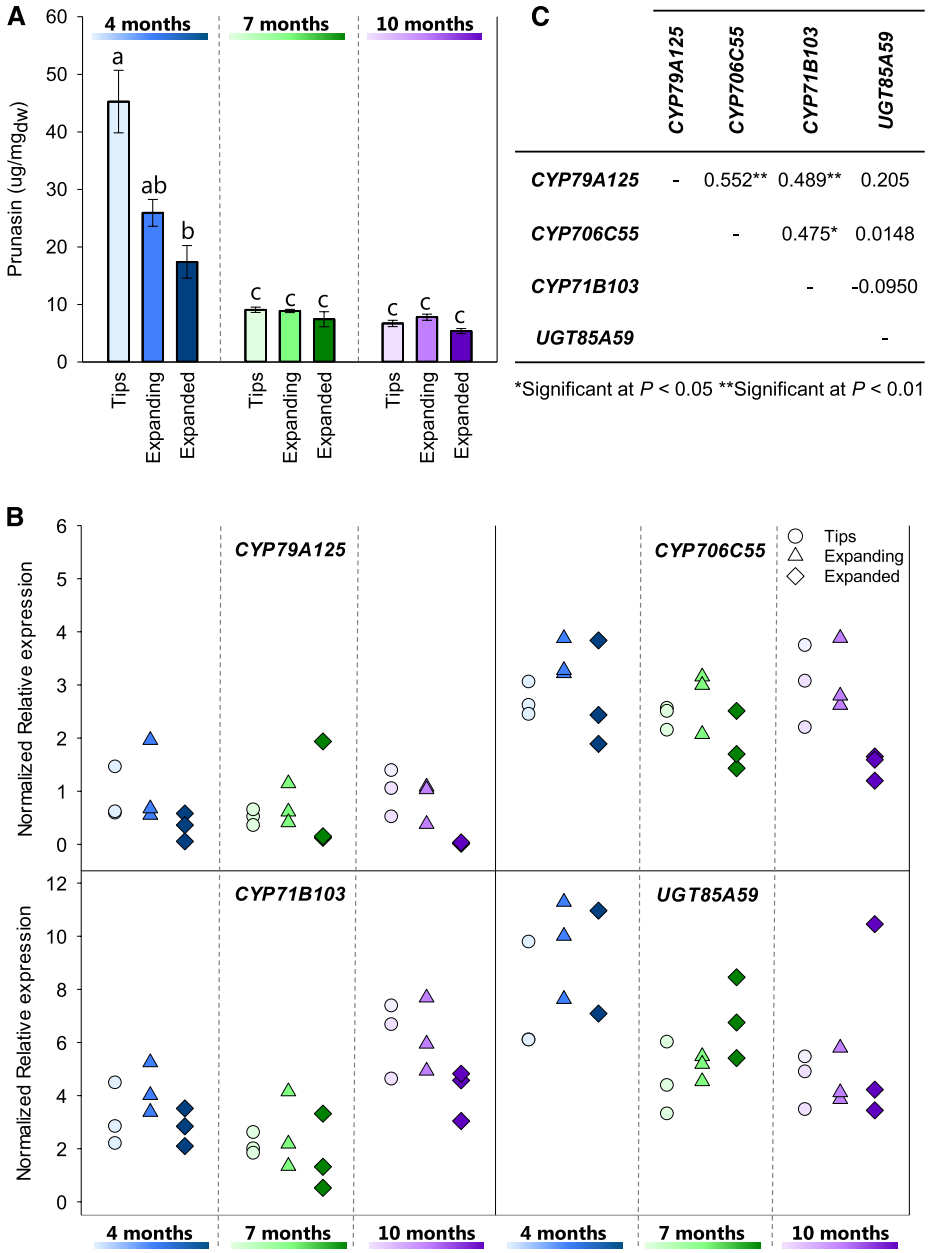

Figure 6. Prunasin accumulation and expression of the biosynthetic genes in 4-, 7-, and 10-month-old *E. cladocalyx* plants (n = 6–8). A, Prunasin accumulation in apical tips, expanding leaves, and expanded leaves. Bars represent means ± SE. Letters denote significance at $P < 0.05$ by one-way ANOVA. dw, Dry weight. B, Normalized gene expression of *CYP79A125*, *CYP706C55*, *CYP71B103*, and *UGT85A59* in apical tips, expanding leaves, and expanded leaves. Symbols represent biological replicates (n = 3). C, Spearman correlation analysis of gene expression showing the coregulation of some genes.

prunasin accumulation declined with age (Goodger et al., 2007). The species-specific differences in the onset of cyanogenic glucoside production provide a unique experimental system for studying the role and regulation of cyanogenic glucoside biosynthesis.

The high concentration of cyanogenic glucosides in young plants, apical tips, and reproductive tissue of *E. cladocalyx* is in accordance with the optimal defense theory of plant defense, whereby the most vulnerable and important structures are the most highly defended (Rhoades, 1979). These results support the general role of cyanogenic glucosides as chemical defense compounds against generalist herbivores and pathogens (Gleadow and Woodrow, 2002). In recent years, it has become apparent that cyanogenic glucosides perform additional roles in plant metabolism, for example, as storage molecules or in quenching reactive oxygen species (Gleadow and Møller, 2014; Schmidt

et al., 2018a). Enzymes and intermediates in the endogenous recycling of autotoxic cyanogenic glucosides, including prunasin and amygdalin, have been identified (Jenrich et al., 2007; Pičmanová et al., 2015; Bjarnholt et al., 2018). Tissue-based localization studies using MALDI-MSI provide important information to aid the understanding of specialized metabolite multifunctionality in planta (Bjarnholt et al., 2014; Boughton et al., 2016). Using MALDI-MSI, we show that prunasin is localized to the mesophyll and vascular tissue of seedling and adult *E. cladocalyx* leaves (Fig. 2, A and B). The localization of prunasin in the vascular tissue of *E. cladocalyx* leaves suggests the transport of cyanogenic glucosides within the plant. The transport of cyanogenic glucosides is known in other cyanogenic species, including cassava (Jørgensen et al., 2005), *Hevea brasiliensis* (Selmar et al., 1988; Selmar, 1993), and sorghum (Selmar et al., 1996; Darbani et al., 2016). Once transported, it is hypothesized that the cyanogenic glucoside is recycled and provides a source of reduced carbon and nitrogen (Pičmanová et al., 2015; Bjarnholt et al., 2018).

MALDI-MSI of the *E. cladocalyx* flower bud revealed distinct patterns of prunasin and amygdalin localization. Prunasin was distributed widely throughout the ground tissue of the ovary, hypanthium, and operculum and was present in the filaments and anthers (Fig. 2, C and D), consistent with a role in chemical defense. Amygdalin colocalized with prunasin but was restricted specifically to the filaments and around the staminal ring region (Fig. 2, C and D). In other species, cyanogenic diglycosides are suggested to be the transport form (Selmar, 1993; Selmar et al., 1996; Neilson et al., 2011), and the results here may suggest the transport of cyanogenic glucosides from the hypanthium to the stamens. The role of cyanogenic glucosides in flower parts has received little attention (Lai et al., 2015). Cyanogenic glucosides have been detected previously in the pollen of almond flowers (London-Shafir et al., 2003; Del Cueto et al., 2017), where they are hypothesized to act as a chemical deterrent to inefficient pollinators. Other specialized metabolites, such as flavonol glycosides, provide a critical role in pollen development, thermotolerance, and reactive oxygen species protection (Paupière et al., 2014). With their multiple functions in plants, investigations into the role of cyanogenic glucosides in *Eucalyptus* flowers would be an intriguing avenue of research.

Recruitment of CYP706C55 Involves an Additional Free Nitrile Intermediate in Prunasin Synthesis

We have identified and characterized three CYPs and a UGT from *E. cladocalyx* catalyzing the formation of prunasin. Similar to other known cyanogenic glucoside biosynthetic pathways, the first step of prunasin biosynthesis in *E. cladocalyx* is catalyzed by a multifunctional CYP79 that converts an amino acid into an aldoxime. The following conversion of the aldoxime into a cyanohydrin requires two CYPs in *E. cladocalyx* instead of a single multifunctional CYP. CYP706C55 converts phenylacetaldoxime into phenylacetonitrile, which is subsequently hydroxylated by CYP71B103 to form mandelonitrile. This is in contrast to the well-characterized dhurrin biosynthesis in sorghum, where CYP71E1 catalyzes a rearrangement of (*E*)-*p*-hydroxyphenylacetaldoxime to (*Z*)-*p*-hydroxyphenylacetaldoxime, then a dehydration of (*Z*)-*p*-hydroxyphenylacetaldoxime to *p*-hydroxyphenylacetonitrile, followed by a *C*-hydroxylation resulting in *p*-hydroxymandelonitrile (Kahn et al., 1997, 1999; Bak et al., 1998; Clausen et al., 2015). In prunasin-producing *Prunus* species, the conversion of phenylacetaldoxime to mandelonitrile likewise is catalyzed by a single CYP71 (Yamaguchi et al., 2014). The small amount of prunasin observed from *N. benthamiana* leaves expressing *CYP79A125*, *CYP706C55*, and *UGT85A59* could imply that an endogenous *N. benthamiana* enzyme can hydroxylate phenylacetonitrile or that CYP706C55 has minor hydroxylation activity. However, mandelonitrile was not observed as a product in microsomes containing CYP79A125 and CYP706C55.

The involvement of an extra CYP in prunasin biosynthesis in *E. cladocalyx* supports the hypothesis that cyanogenic glucoside biosynthesis has evolved independently in several plant lineages. This hypothesis is exemplified by the identification and characterization of *L. japonicus* CYP736A2 in lotaustralin and linamarin biosynthesis (Takos et al., 2011). Differences in the biosynthesis of hydrogen cyanide-based defenses also are known from outside the plant kingdom. In 2010, it was shown that cyanogenic glucoside biosynthesis in plants and insects evolved independently; in the burnet moth (*Zygaena filipendulae*), linamarin and lotaustralin are produced by two CYPs (CYP405A2 and CYP332A3) and a glucosyltransferase (UGT33A1; Jensen et al., 2011). The number of enzymes required for the production of the cyanohydrin also may differ in insects. The millipede *Chamberlinius hualienensis* produces mandelonitrile as a precursor substrate for its hydrogen cyanide-based defense, and recently, a CYP (CYP320B1) was shown to hydroxylate phenylacetonitrile to form mandelonitrile (Yamaguchi et al., 2017). This function is similar to that of CYP71B103 reported here and indicates that the production of α-hydroxynitriles for hydrogen cyanide defense in some insects also might involve three CYPs.

The three-CYP system in prunasin biosynthesis in *E. cladocalyx* presented here comprises an additional intermediate that needs to be channeled between enzymes for the production of prunasin compared with the two-CYP system in other cyanogenic species. Interestingly, the volatile intermediate phenylacetonitrile is produced and released in some plant species in response to herbivory. For example, the production of herbivore-induced volatiles including phenylacetonitrile has been reported for western balsam poplar (*Populus trichocarpa*; Irmisch et al., 2013), black poplar (*Populus nigra*; McCormick et al., 2014), and giant knotweed (*Fallopia sachalinensis*; Noge et al., 2011). It

can be speculated whether some *Eucalyptus* species might produce and release herbivore-induced nitriles. To our knowledge, however, the emission of these volatile compounds has not been reported for *Eucalyptus* species.

Interestingly, CYPs from different families have acquired the ability to produce phenylacetonitrile from phenylacetaldoxime. In *E. cladocalyx*, CYP706C55 from the CYP706 family catalyzes this reaction, whereas *P. trichocarpa* and *F. sachalinensis* possess CYPs belonging to the large and functionally diverse CYP71 family that convert phenylacetaldoxime into phenylacetonitrile (Irmisch et al., 2014; Yamaguchi et al., 2016; Fig. 5; Supplemental Table S1). Phylogenetically, the *E. cladocalyx* CYP71B103 that hydroxylates phenylacetonitrile groups together with the *P. trichocarpa* CYP71s. These examples of functional diversity within CYP families, together with the examples of independent evolution of cyanogenic glucoside biosynthesis in plants, suggest that it is sometimes necessary to move away from phylogeny for the identification of CYP enzymes involved in the biosynthetic pathway of interest. In contrast, the reactions catalyzed by the CYP79 family are more conserved, as they all convert an amino acid into its corresponding oxime (Sørensen et al., 2018).

CYP706C55 Catalyzes an Atypical CYP Reaction

CYP706C55 was identified as the second enzyme in the prunasin biosynthetic pathway in *E. cladocalyx*. Three CYP706 members from other plant species have been functionally characterized previously and demonstrated to catalyze oxygenation reactions: CYP706B1 from cotton (*Gossypium arboruem*; Luo et al., 2001), CYP706M1 from Alaska cedar (*Callitropsis nootkatensis*), and a CYP706X from *Erigeron breviscapus* (Liu et al., 2018). In contrast, CYP706C55 catalyzes an unusual CYP reaction, which is the dehydration of phenylacetaldoxime to phenylacetonitrile. Although this is an unusual CYP reaction, CYP-catalyzed dehydration of an oxime to its corresponding nitrile has been characterized before for human CYP3A4 (Boucher et al., 1994), Arabidopsis (*Arabidopsis thaliana*) CYP71A13 (Nafisi et al., 2007), *P. trichocarpa* CYP71B40v3 and CYP71B41v2 (Irmisch et al., 2014), and *F. sachalinensis* CYP71AT96 (Yamaguchi et al., 2016). Dehydration of an aldoxime also is one of the partial reactions catalyzed by the multifunctional CYP71E1 in dhurrin biosynthesis in sorghum, as discussed above. Nonetheless, if CYP71E1 was administered with *p*-hydroxyphenylacetaldoxime in the absence of cytochrome P450 oxidoreductase (POR) and NAPDH, the reaction resulted in the accumulation of *p*-hydroxyphenylacetonitrile (Bak et al., 1998).

Exogenous NADPH and POR are not necessarily needed in in vitro assays for CYP71A13 and CYP71B41v2 to catalyze the formation of indole-3-acetacetonitrile and phenylacetonitrile, respectively (Nafisi et al., 2007; Irmisch et al., 2014). Even though POR may not be required for CYP706C55 catalysis, it has been shown that a reducing environment is needed for the CYP-catalyzed dehydration of oximes (DeMaster et al., 1992; Boucher et al., 1994; Hart-Davis et al., 1998). A reducing environment established by, for example, the addition of NADPH or dithionite to an assay will bring the heme group of the CYP to the Fe(II) state. This enables binding of the aldoxime nitrogen to the heme, which allows for a charge transfer from Fe(II) to the aldoxime C=N bond, favoring elimination of the hydroxy group (Boucher et al., 1994; Hart-Davis et al., 1998).

Regulation of Prunasin Biosynthesis

Prunasin accumulation and gene expression were investigated in 4-, 7-, and 10-month-old *E. cladocalyx* seedlings (Fig. 6). Overall, biological replicates showed a large variation in expression of the pathway genes. Likewise, a large variation in prunasin content also was observed. A great variation in prunasin levels was to be expected from the eight individuals, as studies of a natural population of adult *E. cladocalyx* also showed great variation, with a difference of 2 orders of magnitude in hydrogen cyanide potential detected (Gleadow and Woodrow, 2000a). The expression pattern of the pathway genes in apical tips and expanding and expanded leaves in 4-month-old plants showed less decrease with leaf age than expected based on the observed pattern of prunasin accumulation. However, most plants showed the highest expression of the CYPs in apical tips and expanding leaves at all three time points, and the expression was found to correlate. In contrast, the expression of UGT85A59 did not correlate with any of the CYPs. Similar to these findings, the expression levels of the two CYPs in cyanogenic glucoside biosynthesis in *L. japonicus* both decreased with leaf age, and expression of the UGTs, which catalyze glucosylation of the cyanohydrins, did not follow the CYP pattern (Takos et al., 2011). *CYP79A125* was the lowest expressed pathway gene and showed the largest relative variation between leaf types (Fig. 6), which may indicate that the first committed step in prunasin biosynthesis controls the overall flux through the pathway. Similarly, the catalytic activity of CYP79A1 constitutes the rate-limiting step in dhurrin biosynthesis in sorghum (Busk and Møller, 2002; Nielsen et al., 2016).

Glucosylation by UGT85A59 Results in Prunasin Formation

Transient expression of *UGT85A59* in *N. benthamiana* showed that UGT85A59 catalyzes glucosylation of the cyanohydrin, resulting in prunasin formation. Consistent with the function of stabilizing the labile cyanohydrin to avoid a toxic release of hydrogen cyanide, *UGT85A59* was the highest expressed pathway gene at most time points (Fig. 6). Since the diglucoside amygdalin was detected in *E. cladocalyx* metabolite extracts (Fig. 1) but not upon transient expression of UGT85A59 in *N. benthamiana*, an additional UGT

remains to be identified that can catalyze a $\beta(1\rightarrow6)$-*O*-glycosylation of prunasin to yield amygdalin. In other cyanogenic plant species, UGT85 members catalyze a monoglucosylation of the cyanohydrins, resulting in the corresponding cyanogenic glucoside (Jones et al., 1999; Franks et al., 2008; Kannangara et al., 2011; Takos et al., 2011). In contrast, less is known about UGTs that catalyze the addition of a second sugar. Recently, two glucosyltransferases, UGT94AF1 and UGT94F2, were shown to glucosylate prunasin to yield amygdalin in almond (Thodberg et al., 2018), and it can be speculated that a UGT94 also catalyzes the glucosylation of prunasin in *E. cladocalyx*.

CONCLUSION

This study has characterized cyanogenic glucoside content and prunasin biosynthesis in *E. cladocalyx*. The monoglucoside prunasin is the major cyanogen in all tissues, although significant levels of the diglucoside amygdalin were detected in the reproductive organs. Until now, all characterized biosynthetic pathways of cyanogenic glucosides in higher plants consisted of two CYP-catalyzed reactions followed by a final glucosylation reaction. Here, we show by biochemical characterization that prunasin production in *E. cladocalyx* is catalyzed by three CYPs from different families and a glucosyltransferase. Notably, the second biosynthetic step is catalyzed by a CYP706, a CYP family not reported previously to participate in the biosynthesis of cyanogenic glucosides. This finding represents a unique example of convergent evolution in the biosynthesis of cyanogenic glucosides in plants.

MATERIALS AND METHODS

Plant Material

Eucalyptus cladocalyx (sugar gum) seeds from a single maternal tree were purchased from the CSIRO Australian Tree Seed Centre. Seedlings for the ontogenetic study were germinated in the glasshouse at the University of Copenhagen on August 24, 2013, and grown at a minimum 22°C during the day (10 h of light) and a minimum 19°C at night and harvested 4, 7, and 10 months after sowing (110, 215, and 285 d after sowing, respectively). At each time point, eight biological replicates were sampled and used for metabolite and RNA extraction. Plant material for transcriptomic sequencing likewise was grown in the glasshouse at the University of Copenhagen. Apical tips from six individual 8-month-old *E. cladocalyx* seedlings were harvested, combined, and snap frozen in liquid nitrogen. Seedlings for MALDI-MSI imaging were germinated in the glasshouse at the University of Melbourne on September 10, 2014, and were grown at an average temperature of 23.3°C ± 1.3°C during the day and 19.6°C ± 1.5°C at night. *E. cladocalyx* expanded adult leaves, immature and mature flower buds, flowers, and young fruit were harvested from three trees growing at the University of Melbourne Parkville Campus (37.7964° S, 144.9612° E, January 2015), the Royal Botanic Gardens (37.8304° S, 144.9796° E, February 2015), and the University of Melbourne Creswick Campus (37.4221° S, 143.8992° E, February 2015). Samples were embedded and frozen on site for MALDI-MSI analysis. Samples for LC-MS were frozen in liquid nitrogen and stored at –80°C until extraction.

Metabolite Extraction and LC-MS

Metabolites from *E. cladocalyx* (15–50 mg of homogenized tissue) were extracted with cold aqueous 80% (v/v) methanol (MeOH). Leaf metabolites from infiltrated *N. benthamiana* plants expressing different combinations of gene candidates were extracted with cold aqueous 85% MeOH from leaf discs (1.5 cm in diameter) harvested 5 d after infiltration. All plant tissue was incubated on ice in cold MeOH for 5 min, and extracts were centrifuged subsequently (3 min, 10,000*g*, 4°C) to sediment plant tissue. Extracts were diluted five times in MilliQ water and filtered through a Durapore membrane (22-µm pore size; Merck Millipore) before injection into an Agilent 1100 Series LC system coupled to a Bruker HCT-Ultra ion-trap mass spectrometer with an electrospray ionization source run in positive mode. Metabolites were separated on a Zorbax SB-C18 column (2.1 × 50 mm, 1.8 µm; Agilent) at 35°C, applying a flow rate of 0.2 mL min^{-1}. The mobile phase A consisted of 0.1% (v/v) HCOOH and 50 µM NaCl, and phase B consisted of 0.1% HCOOH in acetonitrile. The first interval was 0 to 0.5 min isocratic with 2% B followed by two consecutive linear gradients: 0.5 to 7.5 min, 2% to 40% B, and 7.5 to 8.5 min, 40% to 90% B, followed by a second isocratic interval of 8.5 to 11.5 min, 90% B. The mobile phase was returned to 2% B from 11.5 to 18 min. The flow rate was raised to 0.3 mL min^{-1} in the interval 11.5 to 13.5 min. LC-MS data were analyzed using Bruker Data Analysis 4.0 software.

MALDI-MSI and Sample Preparation

MALDI-MSI was carried out according to Schmidt et al. (2018b). In short, the first fully expanded leaf of *E. cladocalyx* seedlings (139 days after sowing), fully expanded leaves from adult trees, and flower buds were embedded in denatured albumin (boiled egg white) and gently frozen over a bath of liquid nitrogen. Albumin-embedded tissue was cryosectioned (30 µm; Leica CM3050 S cryostat; Leica Microsystems), mounted onto double-sided carbon tape attached to glass slides, and freeze dried overnight. 2,5-Dihydroxybenzoic acid was used as the matrix and sublimated onto tissue sections using a custom-built sublimation apparatus. MS images were acquired in positive ion mode using a Bruker SolariX XR 7-Tesla Hybrid ESI/MALDI-FT-ICR-MS apparatus (Bruker Daltonik).

A mass range of 100 to 2,000 *m/z* was employed, with the instrument set to broadband mode with a time domain for acquisition of 2M, providing an estimated resolving power of 130,000 at *m/z* 400. The laser was set to 30% to 45% power using the minimum spot size (laser spot size approximately 10 × 15 µm), smart-walk selected, and random raster enabled, resulting in ablation spots of approximately 35 to 40 µm in diameter; a total 1,500 to 2,000 shots were fired per spectrum at a frequency of 2 kHz within a 40 × 40 µm array. Optical images of tissue sections were acquired using an Epson Photosmart 4480 flatbed scanner using a minimum setting of 4,800 dots per inch. Optical images are presented as an inverted image, generated in Adobe Photoshop CS2 (Adobe). The data were analyzed using Compass FlexImaging 4.1 (Bruker), data were normalized using root mean square normalization, and individual ion images were scaled as a percentage of maximum signal intensity to enhance visualization. Potassium adducts of prunasin ($[M+K]^+$ *m/z* 334.0691, calculated 334.0687, 1.2 ppm error) and amygdalin ($[M+K]^+$ *m/z* 496.1202, calculated 496.1216, 2.6 ppm error) were compared with authentic standards, spotted, and dried onto a separate glass slide.

Characterization of the *E. cladocalyx* Cyanogenic Glucoside Biosynthetic System

To test the substrate, product, and biosynthetic capacity, *E. cladocalyx* leaves of different developmental stages, newly emerged apical tips and expanding and expanded leaves were harvested from 5-month-old seedlings (biological duplicates) and incubated in L-[^{14}C(U)]-Phe (1.25 mCi, 321 mCi $mmol^{-1}$; Amersham Biosciences, GE Healthcare) and NADPH (0.1 mM) in a total volume of 165 µL for 12 h at room temperature. At the end of incubation, cyanogenic glucosides were extracted in boiling MeOH (80%, 1.5 mL, 5 min), defatted with two extractions using pentane (700 µL), and filtered (0.22 µm low-binding Durapore membrane; Millipore), and 5-µL aliquots were spotted onto a TLC plate (Silica gel60F_{254}, 0.2 mm thickness; Merck), which was developed in EtOAc:HOAc:MeOH:water (16:5:5:2, v/v/v/v). Radioactively labeled cyanogenic glucosides were visualized using a STORM 840 PhosphorImager (Molecular Dynamics) and compared with the position of an unlabeled, coapplied prunasin standard (Møller et al., 2016) visualized by UV absorption.

RNA Extraction

Total RNA was extracted from *E. cladocalyx* leaves (apical tips and expanding and expanded leaves) at three different ages in biological triplicates using the Spectrum Plant Total RNA Kit (Sigma) according to the manufacturer's instructions with a few modifications: approximately 20 mg of homogenized tissue was used for extraction, and centrifugation was carried out at 4°C. DNase treatment was performed using RNase-free DNase I from Omega Biotek. The integrity of RNA was verified on an Agilent 2100 Bioanalyzer instrument using an RNA 6000 Nano Kit (Agilent Technologies) according to the manufacturer's instructions, and quantity was estimated using a NanoDrop ND-1000 spectrophotometer (Saveen Werner).

cDNA Synthesis and Quantitative PCR

cDNA was synthesized from 1.5 µg of RNA using SuperScript IV VILO Master Mix (Invitrogen) according to the manufacturer's instructions. The cDNA was diluted 30 times, and 4 µL was used as a template in the quantitative PCR (total volume, 10 µL) using the SeniFAST SYBR No-ROX Kit (Bioline) and gene-specific primers (final concentration, 0.4 µM). Reactions were carried out in technical triplicates, and triplicate nontemplate controls were included for every primer pair. A serial dilution from a pool of cDNA also was included for all primer pairs to correct for primer efficiency. Reactions were carried out on a CFX384 Touch Real-Time PCR Detection System (Bio-Rad) using two-step cycling parameters: 95°C for 2 min, followed by 45 cycles of 95°C for 5 s and then 60°C for 20 s. Melt-curve analysis was performed by gradually increasing the temperature from 65°C to 95°C with 0.5°C raises. Data were analyzed using Bio-Rad CFX Manager 3.1 and qbase+ version 3.1. Eight candidate reference genes used previously for gene expression analysis in *Eucalyptus* species were selected from the literature, and primers were designed to match nucleotide sequences from our transcriptome (Supplemental Table S2). Eight candidate reference genes were tested for stability on 10 different samples using geNorm (Vandesompele et al., 2002). *tRNA* and *MDH* showed the highest expression stability (Supplemental Fig. S4) and, thus, were used to normalize the expression of the prunasin pathway genes. Primers specific for prunasin pathway transcripts are listed in Supplemental Table S3. Normalized relative quantities were calculated according to Hellemans et al. (2007) by setting $Cq_{reference}$ to 0.

Transcriptome Analysis

RNA extracted from apical tips of *E. cladocalyx* was sent for transcriptomic sequencing (Hiseq2500, 100-bp paired end) by Macrogen. The transcriptome was de novo assembled and functionally classified, and expression levels were quantified by Sequentia Biotech. In brief, reads were quality checked, and low-quality reads were removed using Trimmomatic (version 0.33; Bolger et al., 2014) with a minimum length setting of 30 bp and a minimum quality score of 25. The high-quality reads were de novo assembled using the Trinity pipeline (Haas et al., 2013). Transcripts were translated using Transdecoder with a minimum length of 50 amino acids and annotated by two different approaches: by a BLAST search against a database of Arabidopsis (*Arabidopsis thaliana*) amino acid sequences and Gene Ontology annotated using the InterProScan software (version 5.13.52.0; Jones et al., 2014). To quantify the expression levels, reads were mapped to the assembled transcriptome using STAR (Dobin et al., 2013), and the expression levels were calculated with the software eXpress (version 1.5.1; Roberts and Pachter, 2013).

Cloning of Genes Involved in Prunasin Biosynthesis

CYP79A125 was isolated from *E. cladocalyx* cDNA using primers that were designed based on *CYP79A34* from *Eucalyptus yarraensis*. *CYP71B103* and *UGT85A59* were isolated from *E. cladocalyx* cDNA using degenerate primers that were designed based on the orthologous sequences in the *Eucalyptus grandis* genome available on Phytozome (Goodstein et al., 2012). Gene-specific primers with *att*B overhangs were used subsequently to amplify the open reading frames for Gateway recombination into pDONR207 (Invitrogen). Primer sequences are listed in Supplemental Table S4. *CYP706C55* was ordered as a synthetic gene (GenScript) with a C-terminal strep tag. In addition, the full open reading frame of *CYP706C55* was amplified from cDNA. Candidate genes were cloned into the pJAM1502 expression vector (Luo et al., 2007) by Gateway recombination. Candidate gene sequences in expression constructs were verified by sequencing (EZ-Seq; Macrogen).

Transient Expression in *Nicotiana benthamiana*

Plasmids were introduced into *Agrobacterium tumefaciens* AGL1 (Lazo et al., 1991) by electroporation. Electroporated cells were recovered in yeast extract peptone medium for 2 h at 28°C and selected on yeast extract peptone agar medium containing 25 µg mL^{-1} rifampicin, 50 µg mL^{-1} carbenicillin, and 50 µg mL^{-1} kanamycin. Transformants were grown overnight at 28°C and 225 rpm. Agrobacteria cells were harvested and resuspended in MilliQ water to a final OD_{600} of 1. Equal volumes of agrobacteria suspensions were mixed and introduced into *N. benthamiana* leaves (approximately 4 weeks old) using a blunt syringe. An expression construct carrying the open reading frame of p19 (Hearne et al., 1990) was always coinfiltrated to prevent posttranscriptional gene silencing (Voinnet et al., 1999; Lakatos et al., 2004). Two plants were infiltrated per combination, and infiltrations were repeated to confirm results. After infiltration, the plants were kept in the greenhouse (21°C day/19°C night) until leaf material was harvested.

Microsomal Preparation

Leaves from transiently transformed *N. benthamiana* were harvested 5 d after infiltration. Approximately 6 g of leaves was homogenized with 0.1 g polyvinylpolypyrrolidone g^{-1} fresh weight and 30 mL of buffer (100 mM Tricine [pH 7.9], 250 mM Suc, 50 mM NaCl, 2 mM DTT, and one tablet of cOmplete protease inhibitor cocktail [Roche] per 200 mL of buffer) using a mortar and pestle at 4°C. The homogenate was filtered through two layers of nylon cloth (22 µm pore size). Samples were centrifuged at 15,000*g* for 15 min at 4°C. The supernatant was applied subsequently to ultracentrifugation for 1 h at 164,244*g* at 4°C. The microsomal pellets were washed in buffer and resuspended in 200 µL of resuspension buffer (50 mM Tricine [pH 7.9], 20 mM NaCl, and 2 mM DTT).

Microsomal Assays

The assay reactions (total volume of 25 µL) consisted of 10-µL microsomes, 0.25 µCi of L-[^{14}C(U)]-Phe (specific activity, 487 mCi $mmol^{-1}$, Perkin-Elmer), 1 mM NADPH, and buffer (50 mM Tricine [pH 7.5] and 100 mM NaCl). Reaction mixtures were incubated for 30 min at 30°C and 300 rpm. The reactions were stopped by direct application to a TLC plate (Silica gel $60F_{254}$, 0.2 mm thickness; Merck). Substrate and products were separated using a mobile phase consisting of *n*-pentane:EtOAc:MeOH (16:2:1, v/v/v). The migration of phenylacetaldoxime, phenylacetonitrile, and mandelonitrile was determined by the application of unlabeled authentic standards, which were visualized by their UV absorbance. Analysis of radiolabeled products was carried out by exposure of the TLC plate to a Storage Phosphor Screen (GE Healthcare) for 8 d followed by visualization using a Typhoon TRIO Variable Mode Imager (GE Healthcare).

Phylogenetic Analysis

Named and functionally characterized CYPs from the literature were subjected to phylogenetic analysis together with the CYPs characterized here. Accession numbers and references are listed in Supplemental Table S1. Amino acid sequences were aligned in MEGA7 (Kumar et al., 2016) using MUSCLE with the default setting. A neighbor-joining tree was generated with $n = 1{,}000$ bootstrap replicates.

Statistical Analyses

Metabolite data were analyzed in SigmaPlot (version 13.0) using one-way ANOVA. Normality (Kolmogorov-Smirnov) and equal variance (Brown-Forsythe) were tested to cutoffs of $P > 0.02$ and $P > 0.04$, respectively, and when assumptions were not met, the data were transformed by natural logarithm. Pearson correlation was used to analyze gene expression.

Accession Numbers

Sequence data for the prunasin biosynthetic genes identified in this study can be found in GenBank under the following accession numbers: CYP79A125 (MH974543), CYP706C55 (MH974544), CYP71B103 (MH974545), and UGT85A59 (MH974546).

Supplemental Data

The following supplemental materials are available.

Supplemental Figure S1. Additional LC-MS data for prunasin production in *N. benthamiana*.

Supplemental Figure S2. LC-MS data for glucosylated phenylacetaldoxime.

Supplemental Figure S3. LC-MS data for the malonic acid derivative of prunasin.

Supplemental Figure S4. geNorm analysis of candidate reference gene stabilities.

Supplemental Table S1. Accession numbers and references for sequences used in the phylogenetic analysis.

Supplemental Table S2. Primer sequences and references for tested candidate reference genes.

Supplemental Table S3. Primer sequences used for gene expression analysis of the prunasin pathway genes.

Supplemental Table S4. Cloning primers.

ACKNOWLEDGMENTS

We gratefully acknowledge Dr. Antanas Spokevicius for prepublication access to the transcriptomic results of *E. cladocalyx* and *E. globulus*. Prof. Ian Woodrow is thanked for hosting J.S.F.Z. during her stay at the University of Melbourne. David Vernon is heartily thanked for his generous support of wildlife research and encouragement to early-career scientists.

Received August 13, 2018; accepted September 26, 2018; published October 8, 2018.

LITERATURE CITED

Andersen MD, Busk PK, Svendsen I, Møller BL (2000) Cytochromes P-450 from cassava (Manihot esculenta Crantz) catalyzing the first steps in the biosynthesis of the cyanogenic glucosides linamarin and lotaustralin: cloning, functional expression in Pichia pastoris, and substrate specificity of the isolated recombinant enzymes. J Biol Chem **275**: 1966–1975

Bak S, Kahn RA, Nielsen HL, Møller BL, Halkier BA (1998) Cloning of three A-type cytochromes P450, CYP71E1, CYP98, and CYP99 from Sorghum bicolor (L.) Moench by a PCR approach and identification by expression in Escherichia coli of CYP71E1 as a multifunctional cytochrome P450 in the biosynthesis of the cyanogenic glucoside dhurrin. Plant Mol Biol **36**: 393–405

Bassard JE, Møller BL, Laursen T (2017) Assembly of dynamic P450-mediated metabolons: order versus chaos. Curr Mol Biol Rep **3**: 37–51

Bjarnholt N, Li B, D'Alvise J, Janfelt C (2014) Mass spectrometry imaging of plant metabolites: principles and possibilities. Nat Prod Rep **31**: 818–837

Bjarnholt N, Neilson EHJ, Crocoll C, Jørgensen K, Motawia MS, Olsen CE, Dixon DP, Edwards R, Møller BL (2018) Glutathione transferases catalyze recycling of auto-toxic cyanogenic glucosides in sorghum. Plant J **94**: 1109–1125

Bolger AM, Lohse M, Usadel B (2014) Trimmomatic: a flexible trimmer for Illumina sequence data. Bioinformatics **30**: 2114–2120

Boucher JL, Delaforge M, Mansuy D (1994) Dehydration of alkyl- and arylaldoximes as a new cytochrome P450-catalyzed reaction: mechanism and stereochemical characteristics. Biochemistry **33**: 7811–7818

Boughton BA, Thinagaran D, Sarabia D, Bacic A, Roessner U (2016) Mass spectrometry imaging for plant biology: a review. Phytochem Rev **15**: 445–488

Burchell B, Nebert DW, Nelson DR, Bock KW, Iyanagi T, Jansen PLM, Lancet D, Mulder GJ, Chowdhury JR, Siest G, (1991) The UDP glucuronosyltransferase gene superfamily: suggested nomenclature based on evolutionary divergence. DNA Cell Biol **10**: 487–494

Busk PK, Møller BL (2002) Dhurrin synthesis in sorghum is regulated at the transcriptional level and induced by nitrogen fertilization in older plants. Plant Physiol **129**: 1222–1231

Clausen M, Kannangara RM, Olsen CE, Blomstedt CK, Gleadow RM, Jørgensen K, Bak S, Motawie MS, Møller BL (2015) The bifurcation of the cyanogenic glucoside and glucosinolate biosynthetic pathways. Plant J **84**: 558–573

Coppen JJW (2002) Eucalyptus: The Genus Eucalyptus. Taylor and Francis, London

Darbani B, Motawia MS, Olsen CE, Nour-Eldin HH, Møller BL, Rook F (2016) The biosynthetic gene cluster for the cyanogenic glucoside dhurrin in *Sorghum bicolor* contains its co-expressed vacuolar MATE transporter. Sci Rep **6**: 37079

Del Cueto J, Ionescu IA, Pičmanová M, Gericke O, Motawia MS, Olsen CE, Campoy JA, Dicenta F, Møller BL, Sánchez-Pérez R (2017) Cyanogenic glucosides and derivatives in almond and sweet cherry flower buds from dormancy to flowering. Front Plant Sci **8**: 800

DeMaster EG, Shirota FN, Nagasawa HT (1992) A Beckmann-type dehydration of *n*-butyraldoxime catalyzed by cytochrome P-450. J Org Chem **57**: 5074–5075

Dobin A, Davis CA, Schlesinger F, Drenkow J, Zaleski C, Jha S, Batut P, Chaisson M, Gingeras TR (2013) STAR: ultrafast universal RNA-seq aligner. Bioinformatics **29**: 15–21

Eschler BM, Pass DM, Willis R, Foley WJ (2000) Distribution of foliar formylated phloroglucinol derivatives amongst *Eucalyptus* species. Biochem Syst Ecol **28**: 813–824

Finnemore H, Cox CB (1928) Cyanogenetic glucosides in Australian plants. J Proc R Soc N S W **62**: 369–378

Finnemore H, Reichard SK, Large DK (1935) Cyanogenetic glucosides in Australian plants: *Eucalyptus cladocalyx*. J Proc R Soc N S W **69**: 209–214

Forslund K, Morant M, Jørgensen B, Olsen CE, Asamizu E, Sato S, Tabata S, Bak S (2004) Biosynthesis of the nitrile glucosides rhodiocyanoside A and D and the cyanogenic glucosides lotaustralin and linamarin in *Lotus japonicus*. Plant Physiol **135**: 71–84

Franks TK, Yadollahi A, Wirthensohn MG, Huerin JR, Kaiser BN, Sedgley M, Ford CM (2008) A seed coat cyanohydrin glucosyltransferase is associated with bitterness in almond (*Prunus dulcis*) kernels. Funct Plant Biol **35**: 236–246

Franzmayr BK, Rasmussen S, Fraser KM, Jameson PE (2012) Expression and functional characterization of a white clover isoflavone synthase in tobacco. Ann Bot **110**: 1291–1301

Gleadow RM, Møller BL (2014) Cyanogenic glycosides: synthesis, physiology, and phenotypic plasticity. Annu Rev Plant Biol **65**: 155–185

Gleadow RM, Woodrow IE (2000a) Polymorphism in cyanogenic glycoside content and cyanogenic β-glucosidase activity in natural populations of *Eucalyptus cladocalyx*. Aust J Plant Physiol **27**: 693–699

Gleadow RM, Woodrow IE (2000b) Temporal and spatial variation in cyanogenic glycosides in *Eucalyptus cladocalyx*. Tree Physiol **20**: 591–598

Gleadow RM, Woodrow IE (2002) Constraints on effectiveness of cyanogenic glycosides in herbivore defense. J Chem Ecol **28**: 1301–1313

Gleadow RM, Foley WJ, Woodrow IE (1998) Enhanced CO_2 alters the relationship between photosynthesis and defence in cyanogenic *Eucalyptus cladocalyx* F. Muell. Plant Cell Environ **21**: 12–22

Gleadow RM, Haburjak J, Dunn JE, Conn ME, Conn EE (2008) Frequency and distribution of cyanogenic glycosides in Eucalyptus L'Hérit. Phytochemistry **69**: 1870–1874

Goodger JQD, Ades PK, Woodrow IE (2004) Cyanogenesis in Eucalyptus polyanthemos seedlings: heritability, ontogeny and effect of soil nitrogen. Tree Physiol **24**: 681–688

Goodger JQD, Gleadow RM, Woodrow IE (2006) Growth cost and ontogenetic expression patterns of defence in cyanogenic Eucalyptus spp. Trees (Berl) **20**: 757–765

Goodger JQ, Choo TY, Woodrow IE (2007) Ontogenetic and temporal trajectories of chemical defence in a cyanogenic eucalypt. Oecologia **153**: 799–808

Goodstein DM, Shu S, Howson R, Neupane R, Hayes RD, Fazo J, Mitros T, Dirks W, Hellsten U, Putnam N, (2012) Phytozome: a comparative platform for green plant genomics. Nucleic Acids Res **40**: D1178–D1186

Haas BJ, Papanicolaou A, Yassour M, Grabherr M, Blood PD, Bowden J, Couger MB, Eccles D, Li B, Lieber M, (2013) De novo transcript sequence reconstruction from RNA-seq using the Trinity platform for reference generation and analysis. Nat Protoc **8**: 1494–1512

Hart-Davis J, Battioni P, Boucher JL, Mansuy D (1998) New catalytic properties of iron porphyrins: model systems for cytochrome P450-catalyzed dehydration of aldoximes. J Am Chem Soc **120**: 12524–12530

Hearne PQ, Knorr DA, Hillman BI, Morris TJ (1990) The complete genome structure and synthesis of infectious RNA from clones of tomato bushy stunt virus. Virology **177**: 141–151

Hellemans J, Mortier G, De Paepe A, Speleman F, Vandesompele J (2007) qBase relative quantification framework and software for management and automated analysis of real-time quantitative PCR data. Genome Biol **8**: R19

Irmisch S, McCormick AC, Boeckler GA, Schmidt A, Reichelt M, Schneider B, Block K, Schnitzler JP, Gershenzon J, Unsicker SB, (2013) Two herbivore-induced cytochrome P450 enzymes CYP79D6 and CYP79D7 catalyze the formation of volatile aldoximes involved in poplar defense. Plant Cell **25**: 4737–4754

Irmisch S, McCormick AC, Günther J, Schmidt A, Boeckler GA, Gershenzon J, Unsicker SB, Köllner TG (2014) Herbivore-induced poplar cytochrome P450 enzymes of the CYP71 family convert aldoximes to nitriles which repel a generalist caterpillar. Plant J **80**: 1095–1107

Jenrich R, Trompetter I, Bak S, Olsen CE, Møller BL, Piotrowski M (2007) Evolution of heteromeric nitrilase complexes in Poaceae with new functions in nitrile metabolism. Proc Natl Acad Sci USA **104**: 18848–18853

Jensen NB, Zagrobelny M, Hjernø K, Olsen CE, Houghton-Larsen J, Borch J, Møller BL, Bak S (2011) Convergent evolution in biosynthesis of cyanogenic defence compounds in plants and insects. Nat Commun **2**: 273

Jones PR, Møller BL, Høj PB (1999) The UDP-glucose:p-hydroxymandelonitrile-O-glucosyltransferase that catalyzes the last step in synthesis of the cyanogenic glucoside dhurrin in *Sorghum bicolor*: isolation, cloning, heterologous expression, and substrate specificity. J Biol Chem **274**: 35483–35491

Jones P, Binns D, Chang HY, Fraser M, Li W, McAnulla C, McWilliam H, Maslen J, Mitchell A, Nuka G, (2014) InterProScan **5**: genome-scale protein function classification. Bioinformatics **30**: 1236–1240

Jørgensen K, Bak S, Busk PK, Sørensen C, Olsen CE, Puonti-Kaerlas J, Møller BL (2005) Cassava plants with a depleted cyanogenic glucoside content in leaves and tubers: distribution of cyanogenic glucosides, their site of synthesis and transport, and blockage of the biosynthesis by RNA interference technology. Plant Physiol **139**: 363–374

Jørgensen K, Morant AV, Morant M, Jensen NB, Olsen CE, Kannangara R, Motawia MS, Møller BL, Bak S (2011) Biosynthesis of the cyanogenic glucosides linamarin and lotaustralin in cassava: isolation, biochemical characterization, and expression pattern of CYP71E7, the oxime-metabolizing cytochrome P450 enzyme. Plant Physiol **155**: 282–292

Kahn RA, Bak S, Svendsen I, Halkier BA, Møller BL (1997) Isolation and reconstitution of cytochrome P450ox and in vitro reconstitution of the entire biosynthetic pathway of the cyanogenic glucoside dhurrin from sorghum. Plant Physiol **115**: 1661–1670

Kahn RA, Fahrendorf T, Halkier BA, Møller BL (1999) Substrate specificity of the cytochrome P450 enzymes CYP79A1 and CYP71E1 involved in the biosynthesis of the cyanogenic glucoside dhurrin in *Sorghum bicolor* (L.) Moench. Arch Biochem Biophys **363**: 9–18

Kannangara R, Motawia MS, Hansen NK, Paquette SM, Olsen CE, Møller BL, Jørgensen K (2011) Characterization and expression profile of two UDP-glucosyltransferases, UGT85K4 and UGT85K5, catalyzing the last step in cyanogenic glucoside biosynthesis in cassava. Plant J **68**: 287–301

Koch BM, Sibbesen O, Halkier BA, Svendsen I, Møller BL (1995) The primary sequence of cytochrome P450tyr, the multifunctional *N*-hydroxylase catalyzing the conversion of L-tyrosine to p-hydroxyphenylacetaldehyde oxime in the biosynthesis of the cyanogenic glucoside dhurrin in *Sorghum bicolor* (L.) Moench. Arch Biochem Biophys **323**: 177–186

Külheim C, Padovan A, Hefer C, Krause ST, Köllner TG, Myburg AA, Degenhardt J, Foley WJ (2015) The Eucalyptus terpene synthase gene family. BMC Genomics **16**: 450

Kumar S, Stecher G, Tamura K (2016) MEGA7: Molecular Evolutionary Genetics Analysis version 7.0 for bigger datasets. Mol Biol Evol **33**: 1870–1874

Lai D, Pičmanová M, Abou Hachem M, Motawia MS, Olsen CE, Møller BL, Rook F, Takos AM (2015) Lotus japonicus flowers are defended by a cyanogenic β-glucosidase with highly restricted expression to essential reproductive organs. Plant Mol Biol **89**: 21–34

Lakatos L, Szittya G, Silhavy D, Burgyán J (2004) Molecular mechanism of RNA silencing suppression mediated by p19 protein of tombusviruses. EMBO J **23**: 876–884

Laursen T, Borch J, Knudsen C, Bavishi K, Torta F, Martens HJ, Silvestro D, Hatzakis NS, Wenk MR, Dafforn TR, (2016) Characterization of a dynamic metabolon producing the defense compound dhurrin in sorghum. Science **354**: 890–893

Lazo GR, Stein PA, Ludwig RA (1991) A DNA transformation-competent Arabidopsis genomic library in Agrobacterium. Biotechnology (N Y) **9**: 963–967

Liu X, Cheng J, Zhang G, Ding W, Duan L, Yang J, Kui L, Cheng X, Ruan J, Fan W, (2018) Engineering yeast for the production of breviscapine by genomic analysis and synthetic biology approaches. Nat Commun **9**: 448

London-Shafir I, Shafir S, Eisikowitch D (2003) Amygdalin in almond nectar and pollen: facts and possible roles. Plant Syst Evol **238**: 87–95

Luo J, Nishiyama Y, Fuell C, Taguchi G, Elliott K, Hill L, Tanaka Y, Kitayama M, Yamazaki M, Bailey P, (2007) Convergent evolution in the BAHD family of acyl transferases: identification and characterization of anthocyanin acyl transferases from *Arabidopsis thaliana*. Plant J **50**: 678–695

Luo P, Wang YH, Wang GD, Essenberg M, Chen XY (2001) Molecular cloning and functional identification of (+)-δ-cadinene-8-hydroxylase, a cytochrome P450 mono-oxygenase (CYP706B1) of cotton sesquiterpene biosynthesis. Plant J **28**: 95–104

Mackenzie PI, Bock KW, Burchell B, Guillemette C, Ikushiro S, Iyanagi T, Miners JO, Owens IS, Nebert DW (2005) Nomenclature update for the mammalian UDP glycosyltransferase (*UGT*) gene superfamily. Pharmacogenet Genomics **15**: 677–685

Marsh KJ, Kulheim C, Blomberg SP, Thornhill AH, Miller JT, Wallis IR, Nicolle D, Salminen JP, Foley WJ (2017) Genus-wide variation in foliar polyphenolics in eucalypts. Phytochemistry **144**: 197–207

McCormick AC, Irmisch S, Reinecke A, Boeckler GA, Veit D, Reichelt M, Hansson BS, Gershenzon J, Köllner TG, Unsicker SB (2014) Herbivore-induced volatile emission in black poplar: regulation and role in attracting herbivore enemies. Plant Cell Environ **37**: 1909–1923

Møller BL (2010) Functional diversifications of cyanogenic glucosides. Curr Opin Plant Biol **13**: 338–347

Møller BL, Olsen CE, Motawia MS (2016) General and stereocontrolled approach to the chemical synthesis of naturally occurring cyanogenic glucosides. J Nat Prod **79**: 1198–1202

Myburg AA, Grattapaglia D, Tuskan GA, Hellsten U, Hayes RD, Grimwood J, Jenkins J, Lindquist E, Tice H, Bauer D, (2014) The genome of *Eucalyptus grandis*. Nature **510**: 356–362

Nafisi M, Goregaoker S, Botanga CJ, Glawischnig E, Olsen CE, Halkier BA, Glazebrook J (2007) *Arabidopsis* cytochrome P450 monooxygenase 71A13 catalyzes the conversion of indole-3-acetaldoxime in camalexin synthesis. Plant Cell **19**: 2039–2052

Neilson EH (2012) Characterisation of cyanogenic glucoside synthesis in Eucalyptus. PhD thesis. University of Melbourne, Melbourne, Australia

Neilson EH, Goodger JQ, Motawia MS, Bjarnholt N, Frisch T, Olsen CE, Møller BL, Woodrow IE (2011) Phenylalanine derived cyanogenic diglucosides from *Eucalyptus camphora* and their abundances in relation to ontogeny and tissue type. Phytochemistry **72**: 2325–2334

Nelson DR (2009) The cytochrome p450 homepage. Hum Genomics **4**: 59–65

Nielsen LJ, Stuart P, Pičmanová M, Rasmussen S, Olsen CE, Harholt J, Møller BL, Bjarnholt N (2016) Dhurrin metabolism in the developing grain of *Sorghum bicolor* (L.) Moench investigated by metabolite profiling and novel clustering analyses of time-resolved transcriptomic data. BMC Genomics **17**: 1021

Noge K, Abe M, Tamogami S (2011) Phenylacetonitrile from the giant knotweed, *Fallopia sachalinensis*, infested by the Japanese beetle, *Popillia japonica*, is induced by exogenous methyl jasmonate. Molecules **16**: 6481–6488

Padovan A, Keszei A, Külheim C, Foley WJ (2014) The evolution of foliar terpene diversity in Myrtaceae. Phytochem Rev **13**: 695–716

Paupière MJ, van Heusden AW, Bovy AG (2014) The metabolic basis of pollen thermo-tolerance: perspectives for breeding. Metabolites **4**: 889–920

Pičmanová M, Neilson EH, Motawia MS, Olsen CE, Agerbirk N, Gray CJ, Flitsch S, Meier S, Silvestro D, Jørgensen K, (2015) A recycling pathway for cyanogenic glycosides evidenced by the comparative metabolic profiling in three cyanogenic plant species. Biochem J **469**: 375–389

Rhoades DF (1979) Evolution of plant chemical defense against herbivores. *In* **GA Rosenthal, DH Janzen**, eds, Herbivores: Their Interaction with Secondary Plant Metabolites. Academic Press, New York, pp 3–54

Roberts A, Pachter L (2013) Streaming fragment assignment for real-time analysis of sequencing experiments. Nat Methods **10**: 71–73

Schmidt FB, Cho SK, Olsen CE, Yang SW, Møller BL, Jørgensen K (2018a) Diurnal regulation of cyanogenic glucoside biosynthesis and endogenous turnover in cassava. Plant Direct **2**: e00038

Schmidt FB, Heskes AM, Thinagaran D, Møller BL, Jørgensen K, Boughton BA (2018b) Mass spectrometry based imaging of labile glucosides in plants. Front Plant Sci **9**: 892

Selmar D (1993) Transport of cyanogenic glucosides: linustatin uptake by *Hevea* cotyledons. Planta **191**: 191–199

Selmar D, Lieberei R, Biehl B (1988) Mobilization and utilization of cyanogenic glycosides: the linustatin pathway. Plant Physiol **86**: 711–716

Selmar D, Irandoost Z, Wray V (1996) Dhurrin-6′-glucoside, a cyanogenic diglucoside from *Sorghum bicolor*. Phytochemistry **43**: 569–572

Sørensen M, Neilson EHJ, Møller BL (2018) Oximes: unrecognized chameleons in general and specialized plant metabolism. Mol Plant **11**: 95–117

Spokevicius AV, Tibbits J, Rigault P, Nolin MA, Müller C, Merchant A (2017) Medium term water deficit elicits distinct transcriptome responses in *Eucalyptus* species of contrasting environmental origin. BMC Genomics **18**: 284

Takos AM, Knudsen C, Lai D, Kannangara R, Mikkelsen L, Motawia MS, Olsen CE, Sato S, Tabata S, Jørgensen K, (2011) Genomic clustering of cyanogenic glucoside biosynthetic genes aids their identification in *Lotus japonicus* and suggests the repeated evolution of this chemical defence pathway. Plant J **68**: 273–286

Thodberg S, Cueto JD, Mazzeo R, Pavan S, Lotti C, Dicenta F, Neilson EH, Møller BL, Sánchez-Pérez R (2018) The bedrock of almond bitterness: the amygdalin pathway in almond (Prunus dulcis). **178**:

Tian L, Dixon RA (2006) Engineering isoflavone metabolism with an artificial bifunctional enzyme. Planta **224**: 496–507

Ting HM, Wang B, Rydén AM, Woittiez L, van Herpen T, Verstappen FW, Ruyter-Spira C, Beekwilder J, Bouwmeester HJ, van der Krol A (2013) The metabolite chemotype of *Nicotiana benthamiana* transiently expressing artemisinin biosynthetic pathway genes is a function of CYP71AV1 type and relative gene dosage. New Phytol **199**: 352–366

Vandesompele J, de Preter K, Pattyn F, Poppe B, van Roy N, de Paepe A, Speleman F (2002) Accurate normalization of real-time quantitative RT-PCR data by geometric averaging of multiple internal control genes. Genome Biol3: research0034.1–research0034.11

Vetter J (2017) Plant cyanogenic glycosides. *In* **P Gopalakrishnakone, CR Carlini, R Ligabue-Braun**, eds, Plant Toxins. Springer Nature, The Netherlands, pp 287–317

Voinnet O, Pinto YM, Baulcombe DC (1999) Suppression of gene silencing: a general strategy used by diverse DNA and RNA viruses of plants. Proc Natl Acad Sci USA **96**: 14147–14152

Yamaguchi T, Yamamoto K, Asano Y (2014) Identification and characterization of CYP79D16 and CYP71AN24 catalyzing the first and second steps in L-phenylalanine-derived cyanogenic glycoside biosynthesis in the Japanese apricot, *Prunus mume* Sieb. et Zucc. Plant Mol Biol **86**: 215–223

Yamaguchi T, Noge K, Asano Y (2016) Cytochrome P450 CYP71AT96 catalyses the final step of herbivore-induced phenylacetonitrile biosynthesis in the giant knotweed, *Fallopia sachalinensis*. Plant Mol Biol **91**: 229–239

Yamaguchi T, Kuwahara Y, Asano Y (2017) A novel cytochrome P450, CYP3201B1, is involved in (*R*)-mandelonitrile biosynthesis in a cyanogenic millipede. FEBS Open Bio **7**: 335–347